

Uncovering RL Integration in SSL Loss: Objective-Specific Implications for Data-Efficient RL

Anonymous authors

Paper under double-blind review

Keywords: Data Efficient RL, Self Predictive RL, Self Supervised Learning

Summary

This paper presents a systematic analysis of the role of self-supervised learning (SSL) objectives and their modifications in data-efficient reinforcement learning. We investigate previously undocumented modifications in the Self-Predictive Representations (SPR) (Schwarzer et al., 2020) framework that significantly impact agent performance. We demonstrate that feature decorrelation-based SSL objectives can achieve comparable performance without relying on domain-specific modifications, and show that the impact of these modifications persists even in more advanced models.

By conducting extensive experiments on the Atari 100k benchmark and DeepMind Control Suite, we provide insights into how different SSL objectives and their modifications affect learning efficiency across diverse environments. Our findings reveal that the choice and adaptation of SSL objectives play a crucial role in achieving data efficiency in self-predictive reinforcement learning, with implications for the design of future algorithms in this space.

Contribution(s)

1. We demonstrate that previously undocumented SSL modifications in SPR (Schwarzer et al., 2020) - terminal state masking and prioritized replay weighting - are crucial for performance, with their removal leading to an 18% decrease in IQM score on Atari 100k
Context: These modifications were silently adopted by subsequent work (D’Oro et al., 2023; Nikishin et al., 2022; Schwarzer et al., 2023) and their impact was not previously analyzed
2. We show that the Barlow Twins SSL objective (Zbontar et al., 2021) can come within 5% of SPR’s performance without using domain-specific modifications, and VICReg (Bardes et al., 2021) can match PlayVirtual’s (Yu et al., 2021) performance in continuous control tasks.
Context: Prior work on SSL in reinforcement learning relied heavily on problem-specific modifications to achieve strong performance (Schwarzer et al., 2020; D’Oro et al., 2023; Schwarzer et al., 2023).
3. We establish that the impact of SSL modifications remains proportionally consistent in more sophisticated models, with unmodified versions of SR-SPR and BBF showing similar relative performance degradation despite having base IQM scores 3x and 2x higher than SPR respectively.
Context: Previous work on SR-SPR (D’Oro et al., 2023; Nikishin et al., 2022) and BBF (Schwarzer et al., 2023) did not investigate the role of these modifications in their improved performance.

Uncovering RL Integration in SSL Loss: Objective-Specific Implications for Data-Efficient RL

Anonymous authors

Paper under double-blind review

Abstract

1 In this study, we investigate the effect of SSL objective modifications within the SPR
 2 framework, focusing on specific adjustments such as terminal state masking and pri-
 3 oritized replay weighting, which were not explicitly addressed in the original design.
 4 While these modifications are specific to RL, they are not universally applicable across
 5 all RL algorithms. Therefore, we aim to assess their impact on performance and ex-
 6 plore other SSL objectives that do not accommodate these adjustments like Barlow
 7 Twins and VICReg. We evaluate six SPR variants on the Atari 100k benchmark, in-
 8 cluding versions both with and without these modifications. Additionally, we test the
 9 performance of these objectives on the DeepMind Control Suite, where such modifi-
 10 cations are absent. Our findings reveal that incorporating specific SSL modifications
 11 within SPR significantly enhances performance, and this influence extends to subse-
 12 quent frameworks like SR-SPR and BBF, highlighting the critical importance of SSL
 13 objective selection and related adaptations in achieving data efficiency in self-predictive
 14 reinforcement learning.

1 Introduction

16 Self-supervised learning (SSL) has become increasingly popular in data-efficient reinforcement
 17 learning (RL) due to its benefits in enhancing both efficiency and performance (Schwarzer et al.,
 18 2023; Ye et al., 2021; Hafner et al., 2023; Srinivas et al., 2020; Tomar et al., 2021; Li et al., 2023;
 19 Cagatan & Akgun, 2023). However, the application of SSL methods is often problem/domain-
 20 specific to maximize the performance of the RL agents. Although this approach is rational given the
 21 nature of these methods, it raises questions about generalization and transferability.

22 One of the key challenges in Deep RL is understanding the factors driving performance improve-
 23 ments, whether through hyperparameter tuning or novel algorithmic approaches (Obando-Ceron
 24 et al., 2024). The lack of transparency in hyperparameter selection often causes issues while algo-
 25 rithmic innovations are usually well-documented. However, our study of different SSL objectives
 26 within the Self-Predictive Representations (SPR) framework (Schwarzer et al., 2020) revealed that
 27 the SSL loss used in SPR differs from what is described in the original publication and its following
 28 works (Nikishin et al., 2022; D’Oro et al., 2023; Schwarzer et al., 2023) built upon it. This moti-
 29 vated us to investigate the effects of the undocumented modifications and further evaluate additional
 30 SSL objectives.

31 Unlike conventional SSL methods in RL, which often follow vision pretraining approaches (Chen
 32 et al., 2020) and directly combine SSL and RL losses (Srinivas et al., 2020), SPR modifies the SSL
 33 loss before integrating it with the RL objective. To further clarify, SPR employs the BYOL/SimSiam
 34 (Grill et al., 2020; Chen & He, 2020) auxiliary objective and incorporates two algorithm-specific
 35 adjustments to the SSL objective: (i) masking SSL loss with a boolean non-terminal state matrix
 36 and (ii) applying prioritized replay weighting to the batch loss. Consequently, this poses an essential
 37 question: How do these modifications affect the base performance of SSL objectives in the RL agent,

and can they be effectively applied to other SSL techniques in the RL domain? In addition, could this be a recurring phenomenon across the following models (Nikishin et al., 2022; Schwarzer et al., 2023) that adopt SPR as their baseline?

Concurrently, a plethora of novel self-supervised representation learning objectives has emerged (Zbontar et al., 2021; Bardes et al., 2021; Ozsoy et al., 2022; Caron et al., 2021), demonstrating performance improvements beyond image pretraining (Lee et al., 2023b; Goulão & Oliveira, 2023; Zhou et al., 2022; Ömer Veysel Çağatan, 2024). These objectives, based on feature decorrelation, do not inherently support the modifications used in SPR because the loss is computed along the feature dimension instead of the batch dimension, which we detail in Section 4.

This divergence raises another important question: How do these alternative objectives perform relative to the original SPR without SSL modifications? This inquiry is particularly significant because the information required to modify SSL objectives may not always be available in the environment. Understanding the performance of these unmodified objectives could provide valuable insights into the generalizability and robustness of different SSL approaches in RL contexts. Towards this end, we incorporate Barlow Twins and VICReg SSL objectives within SPR.

In essence, we frame our investigation around the following questions:

1. **How do these modifications affect the performance of SPR, and do their impacts extend to SPR-based models such as SR-SPR and BBF? Additionally, how do these alternative objectives compare to the original SPR when no SSL modifications are implemented?**

Our findings reveal that modifications to SSL significantly affect SPR performance, leading to an 18% decrease in IQM when these modifications are removed. Additionally, SR-SPR and BBF exhibit a similar decline in performance. Among these modifications, prioritized replay weighting stands out as the most influential. Notably, Barlow Twins achieves results comparable to those of the original SPR, while VICReg’s performance aligns with that of prioritized replay weighting. This indicates that these problem-specific modifications can be mitigated by employing alternative SSL objectives. Overall, our results underscore the importance of SSL modifications in SPR, which persist in strong models that utilize SPR

2. **How effectively do these SSL objectives perform in an environment in which SPR modifications are not applicable?**

To address this, we examine VICReg, Barlow Twins, and SPR (BYOL/SimSiam) within the DeepMind Control Suite, where the popular SAC agent does not utilize prioritized replay weighting and the environment lacks a terminal state. Unlike in the Atari 100k benchmark, our results show VICReg as the top performer, even outpacing PlayVirtual, a more sophisticated variant of SPR. Meanwhile, SPR and Barlow Twins exhibit comparable performance levels. These findings highlight that algorithms tailored for specific domains may not consistently excel across different problem sets. Therefore, transferability should be a key factor in the design of new Deep RL algorithms.

2 Related Work

Tomar et al. (2021) tackles a more challenging setting for representation learning within RL with background distractors, using a simple baseline approach that avoids metric-based learning, data augmentations, world-model learning, and contrastive learning. They analyze why previous methods may fail or perform similarly to the baseline in this tougher scenario and stress the importance of detailed benchmarks based on reward density, planning horizon, and task-irrelevant components. They propose new metrics for evaluating algorithms and advocate for a data-centric approach to better apply RL to real-world tasks.

Li et al. (2023) explore whether SSL can enhance online RL from pixel data. By extending the contrastive reinforcement learning framework (Srinivas et al., 2020) to jointly optimize SSL and RL losses, and experimenting with various SSL losses, they find that the current SSL approaches

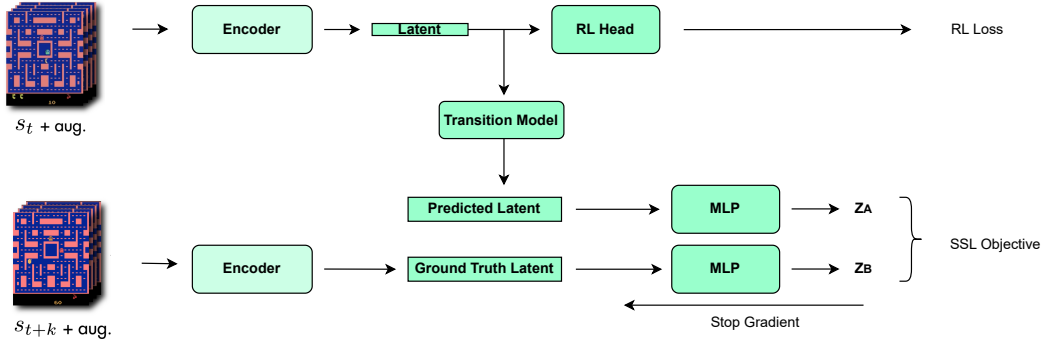


Figure 1: General flow diagram of SPR based methods. An encoder is used to create representations used for reinforcement learning and predicting future representations via a transition model and ground truth representations are created by the same encoder. MLPs differ when the predictor layer is used as in the case of BYOL/SimSiam. While we show the k^{th} step here, the actual loss computation covers steps 1 to K . The SSL objective and RL loss changes between specific methods.

offer no significant improvement over baselines that use image augmentation alone, given the same data and augmentation. Even after evolutionary searches for optimal SSL loss combinations, these methods do not outperform carefully designed image augmentations. Their evaluation across various environments, including real-world robots, reveals that no single SSL loss or augmentation method consistently excels.

2.1 Data Efficient RL in Atari 100k

The introduction of the Atari 100k benchmark (Kaiser et al., 2019) has expedited the advancement of sample-efficient reinforcement learning algorithms. Model-based approach, SimPLe (Kaiser et al., 2019), outperformed Rainbow DQN (Hessel et al., 2017), showcasing superior performance. Building on Rainbow’s framework, Hasselt et al. (2019) enhanced its efficacy through minor hyperparameter adjustments, resulting in Data-Efficient Rainbow (DER), which achieved a higher score compared to SimPLe.

DrQ (Kostrikov et al., 2020) employs a multi-augmentation strategy to regularize the value function during training of both Soft Actor-Critic (Haarnoja et al., 2018) and Deep Q-Network (Mnih et al., 2015). This approach effectively reduces overfitting and enhances training efficiency, leading to performance improvements for both algorithm

Several prevalent methods adopt the Atari 100k dataset, and these can be classified as follows: Model-Based (Hafner et al., 2023; Robine et al., 2023; Micheli et al., 2022; Ayton & Asai, 2021; Robine et al., 2021), Pretraining (Goulão & Oliveira, 2022; Schwarzer et al., 2021b; Lee et al., 2023a; Liu & Abbeel, 2021), Model-Free (Schwarzer et al., 2023; Huang et al., 2022; Nikishin et al., 2022; Cetin et al., 2022a; Lee et al., 2023a; Liang et al., 2022)

2.2 Representation Learning in Atari 100k

Cetin et al. (2022b) presents a deep reinforcement learning method using hyperbolic space for latent representations. Their innovative approach tackles optimization challenges in existing hyperbolic deep learning, ensuring stable end-to-end learning through deep hyperbolic representations.

Huang et al. (2022) proposes a Multiview Markov Decision Process (MMDP) with View-Consistent Dynamics (VCD), a method that enhances traditional MDPs by considering multiple state perspectives. VCD trains a latent space dynamics model for consistent state representations, achieved through data augmentation.

Srinivas et al. (2020) incorporate the InfoNCE (van den Oord et al., 2019) as an auxiliary component within DER. Cagatan & Akgun (2023) uses Barlow Twins (Zbontar et al., 2021) instead of a contrastive objective to further improve results. This integration serves to enhance the learning process. SPR (Schwarzer et al., 2020) outperforms all previous model-free approaches by predicting its latent state representations multiple steps into the future with BYOL (Grill et al., 2020).

PlayVirtual (Yu et al., 2021) introduces a novel transition model as an alternative to the simplistic module in SPR. The methodology enriches actual trajectories by incorporating a multitude of cycle-consistent virtual trajectories. These virtual trajectories, generated using both forward and backward dynamics models, collectively form a closed 'trajectory cycle.' The crucial aspect is ensuring the consistency of this cycle, validating the projected states against real states and actions. This approach significantly improves data efficiency by acquiring robust feature representations with reduced reliance on real-world experiences. This method proves particularly advantageous for tasks where obtaining real-world data is costly or challenging.

3 SPR

SPR is a performant data-efficient agent and a baseline of many other performant agents (Schwarzer et al., 2023; Nikishin et al., 2022; D'Oro et al., 2023; Yu et al., 2021) and its general architecture is depicted in Figure 1. The approach trains an agent by having it predict the latent state based on the current state. It encodes the present state, forecasts the latent representation of the next state using a transition model, and calculates loss by measuring the mean squared error between normalized embeddings. Additionally, SPR adjusts its loss through terminal masking and prioritized replay weighting. These two modifications inject RL-specific information into the auxiliary self-supervised learning task. While the utilization of these ideas is not explicitly mentioned by Schwarzer et al. (2020), it is possible that these techniques were considered self-evident and consequently were included in their implementation (Schwarzer et al., 2021a). We mention them here so as to be able to better differentiate between SPR and other SPR variants.

SSL loss matrix in SPR denoted as L , encompasses negative cosine similarities between predicted latent representations and ground truth latent representations, with dimensions of $B \times (K+1)$, where B is the batch size, and K is the prediction horizon with 1 coming from the current observation. The batch of interactions is drawn from the replay buffer, and their terminal status is known. The terminal mask matrix, M , is composed of 0s and 1s denoting terminal and non-terminal states. The process involves updating L through a Hadamard product with M , denoted as $L \circ M$, effectively modifying the loss matrix.

The loss matrix is divided into two components: SPR loss and Model SPR loss. SPR loss is between the latent representations of the augmented views of the present state. Model SPR loss is between the latent representations of the augmented views of the future states and the predicted future latent representations, generated by the transition model. Model SPR is averaged across the temporal dimension and as a result, both components have $N \times 1$ dimensionality.

The loss of each transition is multiplied by the prioritized replay weight, determined by the temporal difference errors. Then the final loss is computed as the weighted sum of the average SPR loss and half the average of the Model SPR loss across a batch as follows:

$$\mathcal{L}_{SPR} = \frac{1}{N} \sum_{i=1}^N \omega_i (\lambda \text{SPR}_i + \gamma \text{Model SPR}_i) \quad (1)$$

where N is the batch size, ω_i is the priority weight ($\sum_i \omega_i = 1$), and i indexes individual transitions, where λ, γ are hyperparameters.

	Median	IQM	Mean	Opt.Gap
Barlow	0.324	0.320	0.605	0.593
VICReg	0.281	0.289	0.600	0.610
VICReg+Non	0.221	0.279	0.554	0.617
Barlow+Non	-0.009	-0.011	-0.171	1.171
ZeroJump	0.270	0.262	0.528	0.636

Table 1: Human-normalized aggregate metrics in Atari 100k. Scores were collected from 10 random runs.

	Median	IQM	Mean	Opt.Gap
Stop-Grad	0.271	0.303	0.615	0.577
No Stop-Grad	0.266	0.282	0.595	0.611

Table 2: Human-normalized aggregate metrics in Atari 100k by VICReg-High. Scores, collected from 10 random runs to assess the efficacy of including stop-gradient.

157 4 SPR-*

158 Despite variations in SSL objectives and RL algorithms across different benchmarks, the architec-
 159 ture remains largely consistent, as depicted in Figure 1. SPR employs a BYOL (Grill et al., 2020)
 160 objective with a momentum of 1, essentially adopting the SimSiam (Chen & He, 2020) approach.
 161 The primary architectural distinction lies in the inclusion of an extra predictor layer in the online
 162 MLP of BYOL or SimSiam to prevent collapse, a feature omitted in the original Barlow Twins and
 163 VICReg formulations as their objectives inherently mitigate the risk of collapse.

164 **SPR-Nakeds** While SPR demonstrates considerable efficacy, the fundamental question remains
 165 unanswered—what is the impact of pure self-supervised learning and potential adaptations leading
 166 to SPR? Consequently, we introduce SPR-Naked, representing pure SSL. To assess the effects of
 167 prioritized replay weighting and terminal masking, we further establish SPR-Naked+Prio and SPR-
 168 Naked+Non, respectively.

169 In addition to the original SPR and its naked versions, we implement two additional types of agents
 170 with different SSL objectives.

171 **SPR-Barlow** To extend the Barlow Twins to future predictions, we compute individual cross-
 172 correlation matrices for both the current and predicted latent representations at each time step. This
 173 results in a total of $K + 1$ matrices, each with dimensions $d \times d$, where d denotes the embedding
 174 dimension within a single batch. Subsequently, we calculate the loss for each matrix and average
 175 the results. To make it easier to compare, we can define $\overline{\text{SPR Loss}}$ and $\overline{\text{Model SPR Loss}}$ analogously
 176 to their SPR counterparts, where the first is about the current state and the latter is about the future
 177 states. The final loss is then;

$$\mathcal{L}_{\text{SPR-Barlow}} = \overline{\text{SPR}} + \frac{1}{K} \sum_{k=1}^K \overline{\text{Model SPR}}_k \quad (2)$$

178 where K is the number of predicted future observations.

179 **SPR-VICRegs** We employ a parallel procedure as in Barlow Twins for VICReg. We introduce
 180 two variations of VICReg-High and VICReg-Low, featuring high or low covariance weights in the
 181 VICReg loss (Equation 11), while maintaining consistency in other hyperparameters. The primary
 182 objective is to observe the impact of feature decorrelation without inducing model collapse.

183 **Why not employ replay weighting and terminal state masking in Barlow/VICReg?** The key
 184 limitation preventing the use of replay weighting or terminal masking in feature decorrelation-based
 185 methods lies in their reliance on covariance regularization. These methods employ either a cross-
 186 correlation matrix or a covariance matrix, both with dimensions matching the feature dimension.
 187 This structure prohibits applying the weighting of a feature dimension matrix using a batch di-
 188 mension matrix. Consequently, these methods produce a unified loss for the entire batch, unlike
 189 approaches such as BYOL or SimSiam, which generate losses on a per-sample basis.

190 **Why use stop-gradient in Barlow/VICReg?** Barlow Twins and VICReg effectively prevent col-
 191 lapse without resorting to symmetry-breaking architectural techniques such as predictor layers or
 192 stop-gradient mechanisms. While not strictly necessary in this scenario, we choose to include a

stop-gradient due to its empirically observed performance improvement, as depicted in Table 2. A more grounded reason stems from the architectural asymmetry introduced by the transition model. In the absence of a stop-gradient, gradients from the encoder’s upper branch flow through the transition model, whereas gradients from the lower branch directly influence the encoder. This asymmetry can potentially lead to suboptimal encoder updates. Despite collapse avoidance in both cases, the inclusion of a stop-gradient is maintained for its superior performance outcomes.

Why not other objectives? Even though there are newly proposed SSL objectives (Silva et al., 2024; Zhang et al., 2024; Weng et al., 2024), it is impractical to include all objectives in experiments due to limited computational resources and the need to prioritize rigorous evaluation to draw precise conclusions however, we attempt to cover the two main families of SSL methods within SPR. The first is self-distillation, represented by BYOL (Grill et al., 2020) or SimSiam (Chen & He, 2020), which are already incorporated into SPR. The second family includes canonical correlation methods, such as VICReg and Barlow. Another category is Deep Metric Learning, which includes contrastive learning variants (Balestriero et al., 2023). However, we do not separately test contrastive objectives, as they have already been shown to be ineffective in SPR (Schwarzer et al., 2020).

Removing Features with Masking We discussed why post-loss-calculation modifications cannot be applied to objectives that involve components in the feature dimension rather than the batch dimension. However, non-terminal masking can be employed to exclude samples from the batch before calculating the SSL loss. Thus, we masked features during the training of the SPR-VICReg and SPR-Barlow agents, leading to unexpected results. As shown in Table 1, the SPR-Barlow agent performed even worse than the random agent. A likely explanation is that the Barlow Twins’ objective relies on batch normalization to compute the cross-covariance matrix. Since masking causes the batch size to vary dynamically, the batch statistics become inconsistent, adversely affecting the batch normalization process. However, this degradation is not observed to the same extent in the SPR-VICReg agent, as the VICReg objective does not rely on batch normalization.

Continuous Control Formulation Although SPR is created specifically for discrete control, delving into the impact of SSL objectives solely within discrete control domains doesn’t provide a comprehensive understanding. This is why we adopt a parallel setup to that of PlayVirtual (Yu et al., 2021), where they establish an SPR-like scheme referred to as SPR[†] as a baseline for continuous control. They utilize the soft actor-critic algorithm (Haarnoja et al., 2018), instead of q-learning due to the continuous nature of the actions. They do not use terminal state masking (since terminal states for control problems are target states) and prioritized replay weighting (since they use a uniform buffer). This shows the importance of generally applicable auxiliary tasks for data-efficient RL.

We evaluate PlayVirtual and SPR[†] from scratch since we were not able to replicate Yu et al. (2021)’s results, potentially due to different benchmark versions. Furthermore, we assess the performance of VICReg-High and Barlow Twins within the SPR[†] configuration. We exclude VICReg-Low in this setting due to the minimal performance difference observed in Atari.

Finally, we explore the potential impact of incorporating the predictor network into Barlow Twins and VICReg, even though they inherently do not need it to prevent dimension collapse. Although the addition of a predictor network is novel in Barlow Twins, VICReg becomes similar to the SPR with this addition like SPR with variance-covariance regularization. The decision to refrain from conducting similar experiments in Atari stems from the substantially higher experimental costs, which are at least 10 times greater than those in the control setting.

5 Evaluation Setup

5.1 Benchmarking: Rliable Framework

Agarwal et al. (2021) discusses the limitations of using mean and median scores as singular estimates in RL benchmarks and highlights the disparities between conventional single-point estimates and

the broader interval estimates, emphasizing the potential ramifications for benchmark dependability and interpretation. In alignment with their suggestions, we provide a succinct overview of human-normalized scores, furnished with stratified bootstrap confidence intervals, in Figures 2 and 3.

5.2 Atari 100k

We assess the SPR framework in a reduced-sample Atari setting, called the Atari 100k benchmark (Kaiser et al., 2019). In this setting, the training dataset comprises 100,000 environment steps, which is equivalent to about 400,000 frames or slightly under two hours of equivalent human experience. This contrasts with the conventional benchmark of 50,000,000 environment steps, corresponding to approximately 39 days of accumulated experience.

The main metric for this setting, widely acknowledged for assessing performance in the Atari 100k context, is the human-normalized score. This measure is mathematically defined as in equation 3, where random score pertains to outcomes achieved through a random policy and the human score is derived from human players (Wang et al., 2015).

$$\frac{score_{\text{agent}} - score_{\text{random}}}{score_{\text{human}} - score_{\text{random}}} \quad (3)$$

5.3 Deep Mind Control Suite

In the Deep Mind Control Suite (Tassa et al., 2018), the agent is configured to function solely based on pixel inputs. This choice is justified by several reasons: the environments involved offer a reasonably challenging and diverse array of tasks, the sample efficiency of model-free reinforcement learning algorithms is notably low when operating directly from pixels in these benchmarks and the performance on the DM control suite is comparable to the context of robot learning in real-world benchmarks.

We use the following six environments (Yarats et al., 2020) for benchmarking: ball-in-cup, finger-spin, reacher-easy, cheetah-run, walker-walk and cartpole-swingup, for 100k steps each.

6 Results and Discussion

6.1 Atari 100k

We mainly investigate the following new SPR models, along with the original SPR: (i) SPR-Naked, featuring no modifications, (ii) SPR-Naked+Non, incorporating terminal masking, (iii) SPR-Naked+Prio, integrating prioritized replay weighting, (iv) SPR-Barlow, (v) SPR-VICReg-High, characterized by a high covariance weight, and (vi) SPR-VICReg-Low, characterized by a low covariance weight. Moreover, we discuss SR-SPR and BBF with their no modifications versions.

Figure 2 shows the performance of the seven agents in the Atari 100k benchmark, calculated using the reliable framework (Agarwal et al., 2021). The individual game performances are given in Appx. 11 and we describe evaluation setup in Section 5.

SPR and SSL Modifications. The original SPR-agent performs the best (top row of Fig. 2). The modifications to the SPR’s SSL objective (see Section 3) have significant impact on the performance but they are not mentioned in the relevant papers (SPR (Schwarzer et al., 2020), SR-SPR (D’Oro et al., 2023; Nikishin et al., 2022), or BBF (Schwarzer et al., 2023)). The no modifications version, SPR-Naked, performs the worst with a nearly 20% performance drop based on the IQM score (last row of Fig. 2). This is crucial because such modifications may not be suitable for all problem domains, which limits their transferability and generalizability. On the other hand, the role of terminal masking and prioritized replay weighting in SPR is especially interesting, as they help boost performance in situations where pure representation learning struggles.

Incorporating prioritized replay weights has a positive effect on SPR (5th row of Fig. 2). These weights act as markers for Bellman errors that mirror the agent’s Q-value approximation perfor-

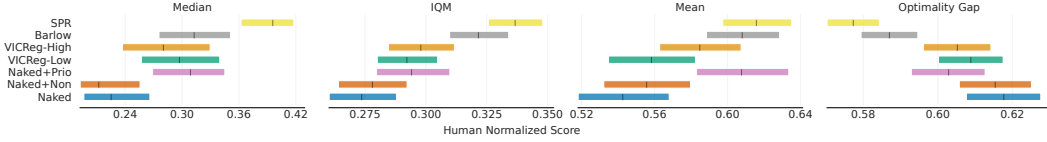


Figure 2: Mean, median, interquartile mean human normalized scores and optimality gap (lower is better) computed with stratified bootstrap confidence intervals in Atari 100k. 50 runs for SPR-Barlow, SPR-VICReg-High, SPR-VICReg-Low, SPR-Naked+Prio, SPR-Naked+Non, SPR-Naked, 100 runs for SPR from (Agarwal et al., 2021).

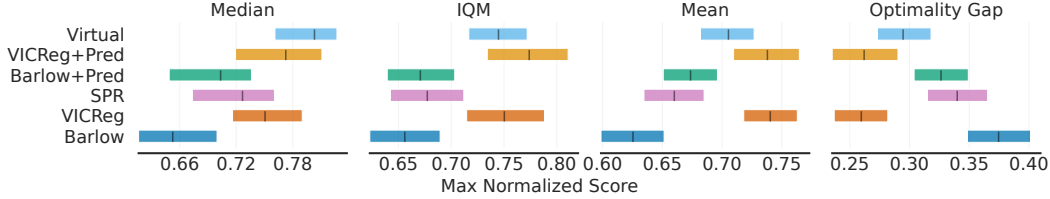


Figure 3: Mean, median, interquartile mean max normalized scores and optimality gap (lower is better) computed with stratified bootstrap confidence intervals in Deep Mind Control Suite 100k, 10 runs for all agents.

284 mance on particular transitions. Introducing these weights into the representation loss intensifies the
 285 emphasis on refining representations that the agent struggles with.

286 Empirically, terminal state masking shows negligible positive effects, unlike replay weighting, (6th
 287 row of Fig. 2). The limited impact of masking might be attributed to the episode lengths, where
 288 the agent encounters many regular states but only a single terminal state. The SSL loss may be
 289 primarily influenced by intermediate states, which could reduce the effectiveness of masking in
 290 these scenarios.

291 On the other hand, there is a clear synergy between these modifications within SPR. Masking termi-
 292 nal states might be advantageous when agents encounter frequent failures during the initial stages
 293 of training or due to the nature of the games. In such cases, terminal states may dominate the replay
 294 buffer, which could introduce biased representations that become challenging to correct later on and
 295 make it harder for the agent to adapt and improve as it progresses

296 **SPR-Barlow.** The performance of the Barlow Twins agent is close to the SPR’s (2nd row of Fig. 2),
 297 with only a 5% difference, whereas SPR-Naked has a 20% gap. As described in Section 4, mod-
 298 ifications related to SSL do not directly apply to Barlow Twins, VICReg, or any other method
 299 regularization in the feature dimension. As such, performing similar to a method with RL specific
 300 modifications suggests that Barlow Twins has the potential to serve as a substitute, indicating its
 301 promise as a versatile SSL objective for data-efficient RL.

302 The performance gap between SPR-naked and the feature decorrelation methods (Barlow and VI-
 303 CReg) in this context is somewhat surprising since BYOL or SimSiam outperform them in image
 304 classification. In vision pretraining, the goal is to obtain embeddings with well-defined clusters
 305 based on the training corpora, enhancing classification performance, where feature decorrelation
 306 may be of hindrance. In RL, it is important to differentiate between states (good, bad, or promising
 307 if they have not been explored yet) which may not be too different in the image space. As such,
 308 methods that emphasize the use of the entire embedding space potentially have a better chance of
 309 state separation.

310 To test this, we evaluate the rank (Kumar et al., 2021) of the advantage and value heads, as well
 311 as the output of the convolution head, which is shared by both the RL and SSL objectives. We
 312 evaluated multiple methods like Barlow Twins and VICReg, in addition to a variant without SSL

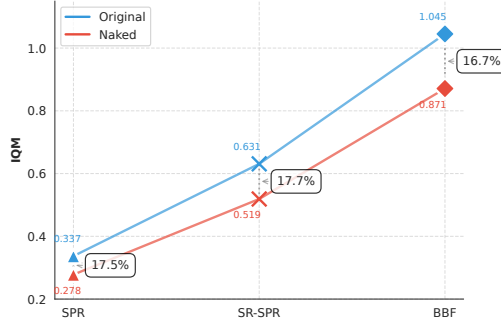


Figure 4: Comparison of IQM performance for the SPR, SR-SPR, and BBF agents alongside their corresponding naked versions. Naked results of SR-SPR and BBF are averaged out across 10 different runs

loss. We found that the rank converges similarly across different games and even if they don’t, this does not correlate with performance. We also measured dormant neurons (Sokar et al., 2023) and observed that the results were consistent with the rank findings. These evaluations are detailed in Appx. 9.

SPR-VICRegs. Initially, we used the default VICReg hyperparameters given in the original paper (Bardes et al., 2021). Surprisingly, VICReg exhibits a 13% lower performance (4th row of Fig. 2) compared to SPR although it surpasses SPR-Naked. It also falls short of Barlow Twins. This outcome is not immediately evident given that it has a high similarity to the Barlow Twins’ objective. One plausible explanation could be the presence of multiple loss components, possibly undermining covariance. To address this, we explore alternative hyperparameters, selecting the set with the highest covariance hyperparameter that avoids collapse and denote it as SPR-VICReg-High, while the previous one is referred to as SPR-VICReg-Low. However, the performance only marginally increases by 2% (3rd row of Fig. 2), lacking behind Barlow Twins once again. The underlying reasons for this performance gap remain subject to further exploration. Nonetheless, it still showcases the effectiveness of feature decorrelation based objectives since both types outperform SPR-Naked.

BBF and SR-SPR. It could be argued that modifications to SPR significantly influence performance, particularly due to its relatively low score on Atari 100k, where such changes may have an amplified effect, whereas they might have a more limited impact on stronger models. BBF, the leading value-based agent achieving human-level results on Atari 100k, is built upon SR-SPR, a variant of SPR. Notably, both SR-SPR and BBF exhibit IQM values nearly 3x and 2x higher than SPR, respectively. Thus, their unmodified results will provide insight into whether modifications still play a significant role, even when the model is highly efficient and performing at a human level.

As shown in Figure 4, we observe that modifications result in a fairly consistent performance decline across all models. Due to computational constraints, we did not conduct experiments to determine which modifications have the greatest impact or whether certain SSL objectives could reduce the need for modifications. However, our findings further support and strengthen our earlier conclusions regarding the impact of modifications on SPR.

6.2 DMControl

We further evaluate the SSL objectives with the DMControl suite, described in Section 5) since this domain can provide additional insights into the efficacy of SSL objectives in RL. However, since there is no terminal state in this environment and a uniform replay buffer is used, modifications to the SPR loss are not feasible. As such, this evaluation will focus on the generalization of used objectives across domains without targeted optimization for specific problems.

Moreover, SPR is not explicitly designed for continuous control. As such, we use a different set of agents modified for continuous control as described in Section 4 but keep the same SSL hyperparameters from the Atari benchmark. We pick SPR-VICReg-High due to its better performance over the lower covariance version. We additionally evaluate SPR-Barlow and SPR-Vicreg with an MLP layer as an additional predictor, reflecting Bardes et al. (2021)’s findings on the enhanced performance of BYOL with variance regularization. We build upon the PlayVirtual (Yu et al., 2021) methodology, which is an SPR equipped with an improved transition model, and use it as our baseline.

We observe from Fig. 3 that the Barlow Twins objective exhibits the lowest performance, although it closely aligns with SPR, with IQM scores of 0.656, and 0.677 respectively. An interesting observation is that VICReg with an IQM of 0.75 is as good as PlayVirtual (Yu et al., 2021) with 0.744. This underscores the potential of SSL objectives in continuous control. While their impact is vital in discrete control as well, the overall effect, especially when considering the maximum score (representing human performance), is relatively modest. Nevertheless, a substantial improvement is evident in continuous control, even when compared to the highest achievable score. We also see that adding a predictor network has a minimal but positive impact on the IQM performances of both Barlow and VICReg.

7 Conclusion

Our study demonstrates the significant impact of SSL objective modifications within the SPR framework for reinforcement learning, particularly in data-efficient scenarios. We show that specific adjustments like terminal state masking and prioritized replay weighting substantially improve performance on the Atari 100k benchmark, with benefits extending to derivative frameworks such as SR-SPR and BBF. However, our experiments on the DeepMind Control Suite reveal that these enhancements are not universally applicable across all RL environments. Investigation of alternative SSL objectives (e.g., Barlow Twins, VICReg) further elucidates the nuanced relationship between objective choice and RL task characteristics. These findings emphasize the critical role of carefully tailored SSL objectives in achieving data efficiency in self-predictive reinforcement learning, highlighting the need for a context-sensitive approach to SSL modification in RL algorithm development. Our work provides valuable insights for researchers and practitioners seeking to optimize RL algorithms across diverse applications, potentially leading to more efficient and effective reinforcement learning systems.

References

- Rishabh Agarwal, Max Schwarzer, Pablo Samuel Castro, Aaron C. Courville, and Marc G. Belle-mare. Deep reinforcement learning at the edge of the statistical precipice. In *Neural Information Processing Systems*, 2021.
- Benjamin J. Ayton and Masataro Asai. Width-based planning and active learning for atari. In *International Conference on Automated Planning and Scheduling*, 2021. URL <https://api.semanticscholar.org/CorpusID:238226837>.
- Randall Balestriero, Mark Ibrahim, Vlad Sobal, Ari Morcos, Shashank Shekhar, Tom Goldstein, Florian Bordes, Adrien Bardes, Gregoire Mialon, Yuandong Tian, Avi Schwarzschild, Andrew Gordon Wilson, Jonas Geiping, Quentin Garrido, Pierre Fernandez, Amir Bar, Hamed Pirsiavash, Yann LeCun, and Micah Goldblum. A cookbook of self-supervised learning, 2023.
- Adrien Bardes, Jean Ponce, and Yann LeCun. Vicreg: Variance-invariance-covariance regularization for self-supervised learning. *ArXiv*, abs/2105.04906, 2021.
- Omer Veysel Cagatan and Baris Akgun. Barlowrl: Barlow twins for data-efficient reinforcement learning, 2023.
- Mathilde Caron, Ishan Misra, Julien Mairal, Priya Goyal, Piotr Bojanowski, and Armand Joulin. Unsupervised learning of visual features by contrasting cluster assignments, 2021.

- 393 Edoardo Cetin, Philip J. Ball, Steve Roberts, and Oya Çeliktutan. Stabilizing off-policy deep rein-
 394 forcement learning from pixels. In *International Conference on Machine Learning*, 2022a. URL
 395 <https://api.semanticscholar.org/CorpusID:250265109>.
- 396 Edoardo Cetin, Benjamin Paul Chamberlain, Michael M. Bronstein, and Jonathan J. Hunt. Hy-
 397 perbolic deep reinforcement learning. *ArXiv*, abs/2210.01542, 2022b. URL <https://api.semanticscholar.org/CorpusID:252693361>.
- 399 Ting Chen, Simon Kornblith, Mohammad Norouzi, and Geoffrey E. Hinton. A simple framework
 400 for contrastive learning of visual representations. *ArXiv*, abs/2002.05709, 2020. URL <https://api.semanticscholar.org/CorpusID:211096730>.
- 402 Xinlei Chen and Kaiming He. Exploring simple siamese representation learning. *2021 IEEE/CVF*
 403 *Conference on Computer Vision and Pattern Recognition (CVPR)*, pp. 15745–15753, 2020.
- 404 Pierluca D’Oro, Max Schwarzer, Evgenii Nikishin, Pierre-Luc Bacon, Marc G. Bellemare, and
 405 Aaron C. Courville. Sample-efficient reinforcement learning by breaking the replay ratio bar-
 406 rier. In *International Conference on Learning Representations*, 2023. URL <https://api.semanticscholar.org/CorpusID:259298604>.
- 408 Manuel Goulão and Arlindo L. Oliveira. Pretraining the vision transformer using self-supervised
 409 methods for vision based deep reinforcement learning. *ArXiv*, abs/2209.10901, 2022. URL
 410 <https://api.semanticscholar.org/CorpusID:252439214>.
- 411 Manuel Goulão and Arlindo L. Oliveira. Pretraining the vision transformer using self-supervised
 412 methods for vision based deep reinforcement learning, 2023.
- 413 Jean-Bastien Grill, Florian Strub, Florent Altch’e, Corentin Tallec, Pierre H. Richemond, Elena
 414 Buchatskaya, Carl Doersch, Bernardo Ávila Pires, Zhaohan Daniel Guo, Mohammad Gheshlaghi
 415 Azar, Bilal Piot, Koray Kavukcuoglu, Rémi Munos, and Michal Valko. Bootstrap your own
 416 latent: A new approach to self-supervised learning. *ArXiv*, abs/2006.07733, 2020. URL <https://api.semanticscholar.org/CorpusID:219687798>.
- 418 Tuomas Haarnoja, Aurick Zhou, P. Abbeel, and Sergey Levine. Soft actor-critic: Off-policy maxi-
 419 mum entropy deep reinforcement learning with a stochastic actor. *ArXiv*, abs/1801.01290, 2018.
 420 URL <https://api.semanticscholar.org/CorpusID:28202810>.
- 421 Danijar Hafner, Jurgis Pasukonis, Jimmy Ba, and Timothy Lillicrap. Mastering diverse domains
 422 through world models. *arXiv preprint arXiv:2301.04104*, 2023.
- 423 H. V. Hasselt, Matteo Hessel, and John Aslanides. When to use parametric models in reinforcement
 424 learning? *ArXiv*, abs/1906.05243, 2019. URL <https://api.semanticscholar.org/CorpusID:186206746>.
- 426 Matteo Hessel, Joseph Modayil, H. V. Hasselt, Tom Schaul, Georg Ostrovski, Will Dabney, Dan
 427 Horgan, Bilal Piot, Mohammad Gheshlaghi Azar, and David Silver. Rainbow: Combining im-
 428 provements in deep reinforcement learning. In *AAAI Conference on Artificial Intelligence*, 2017.
 429 URL <https://api.semanticscholar.org/CorpusID:19135734>.
- 430 Tao Huang, Jiacheng Wang, and Xiao Chen. Accelerating representation learning with view-
 431 consistent dynamics in data-efficient reinforcement learning. *ArXiv*, abs/2201.07016, 2022. URL
 432 <https://api.semanticscholar.org/CorpusID:246035501>.
- 433 Lukasz Kaiser, Mohammad Babaeizadeh, Piotr Milos, Blazej Osinski, Roy H. Campbell,
 434 K. Czechowski, D. Erhan, Chelsea Finn, Piotr Kozakowski, Sergey Levine, Afroz Mohiud-
 435 din, Ryan Sepassi, G. Tucker, and Henryk Michalewski. Model-based reinforcement learning
 436 for atari. *ArXiv*, abs/1903.00374, 2019. URL <https://api.semanticscholar.org/CorpusID:67856232>.

- 438 Ilya Kostrikov, Denis Yarats, and Rob Fergus. Image augmentation is all you need: Regularizing
439 deep reinforcement learning from pixels. *ArXiv*, abs/2004.13649, 2020. URL [https://api.
440 semanticscholar.org/CorpusID:216562627](https://api.semanticscholar.org/CorpusID:216562627).
- 441 Aviral Kumar, Rishabh Agarwal, Dibya Ghosh, and Sergey Levine. Implicit under-parameterization
442 inhibits data-efficient deep reinforcement learning, 2021. URL [https://arxiv.org/abs/
443 2010.14498](https://arxiv.org/abs/2010.14498).
- 444 Hojoon Lee, Hanseul Cho, Hyunseung Kim, Daehoon Gwak, Joonkee Kim, Jaegul Choo, Se-Young
445 Yun, and Chulhee Yun. Enhancing generalization and plasticity for sample efficient reinforcement
446 learning. *ArXiv*, abs/2306.10711, 2023a. URL [https://api.semanticscholar.org/
447 CorpusID:259203876](https://api.semanticscholar.org/CorpusID:259203876).
- 448 Hojoon Lee, Koanho Lee, Dongyoon Hwang, Hyunho Lee, Byungkun Lee, and Jaegul Choo. On
449 the importance of feature decorrelation for unsupervised representation learning in reinforcement
450 learning, 2023b.
- 451 Xiang Li, Jinghuan Shang, Srijan Das, and Michael S. Ryoo. Does self-supervised learning re-
452 ally improve reinforcement learning from pixels?, 2023. URL [https://arxiv.org/abs/
453 2206.05266](https://arxiv.org/abs/2206.05266).
- 454 Litian Liang, Yaosheng Xu, Stephen McAleer, Dailin Hu, Alexander T. Ihler, P. Abbeel, and
455 Roy Fox. Reducing variance in temporal-difference value estimation via ensemble of deep
456 networks. *ArXiv*, abs/2209.07670, 2022. URL [https://api.semanticscholar.org/
457 CorpusID:250341019](https://api.semanticscholar.org/CorpusID:250341019).
- 458 Hao Liu and P. Abbeel. Aps: Active pretraining with successor features. In *International Conference*
459 *on Machine Learning*, 2021. URL [https://api.semanticscholar.org/CorpusID:
460 235825462](https://api.semanticscholar.org/CorpusID:235825462).
- 461 Vincent Micheli, Eloi Alonso, and Francois Fleuret. Transformers are sample efficient world
462 models. *ArXiv*, abs/2209.00588, 2022. URL [https://api.semanticscholar.org/
463 CorpusID:251979354](https://api.semanticscholar.org/CorpusID:251979354).
- 464 Volodymyr Mnih, Koray Kavukcuoglu, David Silver, Andrei A. Rusu, Joel Veness, Marc G. Belle-
465 mare, Alex Graves, Martin A. Riedmiller, Andreas Kirkeby Fiedjeland, Georg Ostrovski, Stig
466 Petersen, Charlie Beattie, Amir Sadik, Ioannis Antonoglou, Helen King, Dharmashan Kumaran,
467 Daan Wierstra, Shane Legg, and Demis Hassabis. Human-level control through deep reinforce-
468 ment learning. *Nature*, 518:529–533, 2015. URL [https://api.semanticscholar.org/
469 CorpusID:205242740](https://api.semanticscholar.org/CorpusID:205242740).
- 470 Evgenii Nikishin, Max Schwarzer, Pierluca D’Oro, Pierre-Luc Bacon, and Aaron C. Courville. The
471 primacy bias in deep reinforcement learning. In *International Conference on Machine Learning*,
472 2022. URL <https://api.semanticscholar.org/CorpusID:248811264>.
- 473 Johan Obando-Ceron, João G. M. Araújo, Aaron Courville, and Pablo Samuel Castro. On the
474 consistency of hyper-parameter selection in value-based deep reinforcement learning, 2024. URL
475 <https://arxiv.org/abs/2406.17523>.
- 476 Serdar Ozsoy, Shadi S. Hamdan, Serkan Ö. Arik, Deniz Yuret, and Alper Tunga Erdogan. Self-
477 supervised learning with an information maximization criterion. *ArXiv*, abs/2209.07999, 2022.
- 478 Jan Robine, Tobias Uelwer, and Stefan Harmeling. Smaller world models for reinforcement learning,
479 2021.
- 480 Jan Robine, Marc Hoftmann, Tobias Uelwer, and Stefan Harmeling. Transformer-based world mod-
481 els are happy with 100k interactions. *ArXiv*, abs/2303.07109, 2023. URL [https://api.
482 semanticscholar.org/CorpusID:257496038](https://api.semanticscholar.org/CorpusID:257496038).

- 483 Max Schwarzer, Ankesh Anand, Rishab Goel, R. Devon Hjelm, Aaron C. Courville, and
 484 Philip Bachman. Data-efficient reinforcement learning with self-predictive representations.
 485 In *International Conference on Learning Representations*, 2020. URL [https://api.](https://api.semanticscholar.org/CorpusID:222163237)
 486 [semanticscholar.org/CorpusID:222163237](https://api.semanticscholar.org/CorpusID:222163237).
- 487 Max Schwarzer, Ankesh Anand, Rishab Goel, R. Devon Hjelm, Aaron C. Courville, and Philip
 488 Bachman. Repository published by the spr. <https://github.com/mila-iqia/spr>,
 489 2021a.
- 490 Max Schwarzer, Nitarshan Rajkumar, Michael Noukhovitch, Ankesh Anand, Laurent Charlin, De-
 491 von Hjelm, Philip Bachman, and Aaron C. Courville. Pretraining representations for data-
 492 efficient reinforcement learning. In *Neural Information Processing Systems*, 2021b. URL
 493 <https://api.semanticscholar.org/CorpusID:235377401>.
- 494 Max Schwarzer, Johan S. Obando-Ceron, Aaron C. Courville, Marc G. Bellemare, Rishabh Agar-
 495 wal, and Pablo Samuel Castro. Bigger, better, faster: Human-level atari with human-level ef-
 496 ficiency. *ArXiv*, abs/2305.19452, 2023. URL [https://api.semanticscholar.org/](https://api.semanticscholar.org/CorpusID:258987895)
 497 [CorpusID:258987895](https://api.semanticscholar.org/CorpusID:258987895).
- 498 Thalles Silva, Helio Pedrini, and Adín Ramírez Rivera. Learning from memory: Non-parametric
 499 memory augmented self-supervised learning of visual features. In Ruslan Salakhutdinov, Zico
 500 Kolter, Katherine Heller, Adrian Weller, Nuria Oliver, Jonathan Scarlett, and Felix Berkenkamp
 501 (eds.), *Proceedings of the 41st International Conference on Machine Learning*, volume 235 of
 502 *Proceedings of Machine Learning Research*, pp. 45451–45467. PMLR, 21–27 Jul 2024. URL
 503 <https://proceedings.mlr.press/v235/silva24c.html>.
- 504 Ghada Sokar, Rishabh Agarwal, Pablo Samuel Castro, and Utku Evci. The dormant neuron phe-
 505 nomenon in deep reinforcement learning, 2023. URL [https://arxiv.org/abs/2302.](https://arxiv.org/abs/2302.12902)
 506 [12902](https://arxiv.org/abs/2302.12902).
- 507 A. Srinivas, Michael Laskin, and P. Abbeel. Curl: Contrastive unsupervised representa-
 508 tions for reinforcement learning. *ArXiv*, abs/2004.04136, 2020. URL [https://api.](https://api.semanticscholar.org/CorpusID:215415964)
 509 [semanticscholar.org/CorpusID:215415964](https://api.semanticscholar.org/CorpusID:215415964).
- 510 Yuval Tassa, Yotam Doron, Alistair Muldal, Tom Erez, Yazhe Li, Diego de Las Casas, David Bud-
 511 den, Abbas Abdolmaleki, Josh Merel, Andrew Lefrancq, Timothy Lillicrap, and Martin Ried-
 512 miller. Deepmind control suite, 2018.
- 513 Manan Tomar, Utkarsh A. Mishra, Amy Zhang, and Matthew E. Taylor. Learning representations
 514 for pixel-based control: What matters and why?, 2021. URL [https://arxiv.org/abs/](https://arxiv.org/abs/2111.07775)
 515 [2111.07775](https://arxiv.org/abs/2111.07775).
- 516 Aaron van den Oord, Yazhe Li, and Oriol Vinyals. Representation learning with contrastive predic-
 517 tive coding, 2019.
- 518 Ziyun Wang, Tom Schaul, Matteo Hessel, H. V. Hasselt, Marc Lanctot, and Nando de Freitas.
 519 Dueling network architectures for deep reinforcement learning. In *International Conference*
 520 *on Machine Learning*, 2015. URL [https://api.semanticscholar.org/CorpusID:](https://api.semanticscholar.org/CorpusID:5389801)
 521 [5389801](https://api.semanticscholar.org/CorpusID:5389801).
- 522 Xi Weng, Yunhao Ni, Tengwei Song, Jie Luo, Rao Muhammad Anwer, Salman Khan, Fahad Shah-
 523 baz Khan, and Lei Huang. Modulate your spectrum in self-supervised learning, 2024. URL
 524 <https://arxiv.org/abs/2305.16789>.
- 525 Denis Yarats, Amy Zhang, Ilya Kostrikov, Brandon Amos, Joelle Pineau, and Rob Fergus. Improv-
 526 ing sample efficiency in model-free reinforcement learning from images, 2020.
- 527 Weirui Ye, Shaohuai Liu, Thanard Kurutach, Pieter Abbeel, and Yang Gao. Mastering atari games
 528 with limited data, 2021.

- 529 Tao Yu, Cuiling Lan, Wenjun Zeng, Mingxiao Feng, Zhizheng Zhang, and Zhibo Chen. Playvirtual:
530 Augmenting cycle-consistent virtual trajectories for reinforcement learning. *Advances in Neural*
531 *Information Processing Systems*, 34, 2021.
- 532 Jure Zbontar, Li Jing, Ishan Misra, Yann LeCun, and Stéphane Deny. Barlow twins: Self-
533 supervised learning via redundancy reduction. *ArXiv*, abs/2103.03230, 2021. URL <https://api.semanticscholar.org/CorpusID:232110471>.
534
- 535 Yifan Zhang, Zhiquan Tan, Jingqin Yang, Weiran Huang, and Yang Yuan. Matrix information theory
536 for self-supervised learning. In Ruslan Salakhutdinov, Zico Kolter, Katherine Heller, Adrian
537 Weller, Nuria Oliver, Jonathan Scarlett, and Felix Berkenkamp (eds.), *Proceedings of the 41st*
538 *International Conference on Machine Learning*, volume 235 of *Proceedings of Machine Learning*
539 *Research*, pp. 59897–59918. PMLR, 21–27 Jul 2024. URL <https://proceedings.mlr.press/v235/zhang24bi.html>.
540
- 541 Jinghao Zhou, Li Dong, Zhe Gan, Lijuan Wang, and Furu Wei. Non-contrastive learning meets
542 language-image pre-training, 2022. URL <https://arxiv.org/abs/2210.09304>.
- 543 Ömer Veysel Çağatan. Unsee: Unsupervised non-contrastive sentence embeddings, 2024. URL
544 <https://arxiv.org/abs/2401.15316>.

Supplementary Materials

The following content was not necessarily subject to peer review.

8 Background

8.1 Barlow Twins

The Barlow Twins (Zbontar et al., 2021) employs a symmetric network with twin branches, each processing a different augmented perspective of input data. It aims to minimize off-diagonal components and align diagonal elements of a cross-covariance matrix derived from the representations of these branches. The process involves generating two altered views (Y^A and Y^B) using data augmentations, inputting them into a function f_θ to produce embeddings (Z^A and Z^B).

The Barlow Twins loss is defined as:

$$\mathcal{L}_{BT} \triangleq \underbrace{\sum_i (1 - C_{ii})^2}_{\text{invariance term}} + \lambda \underbrace{\sum_i \sum_{j \neq i} C_{ij}^2}_{\text{redundancy reduction term}} \quad (4)$$

where $\lambda > 0$ balances the invariance (diagonal elements) and redundancy reduction (off-diagonal) in the loss function. C is the cross-correlation matrix from embedding outputs of identical networks in the batch. A matrix element is defined as:

$$C_{ij} \triangleq \frac{\sum_b z_{b,i}^A z_{b,j}^B}{\sqrt{\sum_b (z_{b,i}^A)^2} \sqrt{\sum_b (z_{b,j}^B)^2}} \quad (5)$$

where b represents the samples in the batch, and i and j represent dimension indices of the networks' output. Each dimension of the square covariance matrix, C , is the same as the embedding dimension (output dimensionality of the networks). Its values range between -1 (indicating complete anti-correlation) and 1 (representing perfect correlation).

8.2 VICReg

VICReg (Bardes et al., 2021) is a method designed to tackle the challenge of collapse directly. It achieves this by introducing a straightforward regularization term that specifically targets the variance of the embeddings along each dimension independently. In addition to addressing the variance, VICReg includes a mechanism to diminish redundancy and ensure decorrelation among the embeddings, accomplished through covariance regularization.

The variance regularization term is a hinge function on the standard deviation of the embeddings along the batch dimension:

$$v(Z) = \frac{1}{d} \sum_{j=1}^d \max(0, \gamma - S(z^j, \epsilon)) \quad (6)$$

where S is the regularized standard deviation defined by:

$$S(x; \epsilon) = \sqrt{\text{Var}(x) + \epsilon} \quad (7)$$

Covariance matrix of Z is defined as:

$$C(Z) = \frac{1}{n-1} \sum_{i=1}^n (z_i - \bar{z})(z_i - \bar{z})^T \quad (8)$$

573 where $\bar{z} = \frac{1}{n} \sum_{i=1}^n z_i$. Covariance regularization is defined as:

$$c(Z) = \frac{1}{d} \sum_i \sum_{j \neq i} c_{ij}^2 \quad (9)$$

574 where d is the feature dimension. The invariance criterion between Z and Z' is the mean-squared
575 Euclidean distance between each pair of vectors, without any normalization.

$$s(Z, Z') = \frac{1}{n} \sum_{i=1}^n \|z_i - z'_i\|^2 \quad (10)$$

576 The overall loss function is a weighted average of the invariance, variance, and covariance terms:

$$l(Z, Z') = \alpha v(Z) + \beta c(Z) + \gamma s(Z, Z') \quad (11)$$

577 where α , λ , and γ hyper-parameters control the importance of each term in the loss.

578 VICReg is quite similar to Barlow Twins in terms of its loss formulation. However, instead of
579 decorrelating the cross-correlation matrix directly, it regularizes the variance along each dimension
580 of the representation, reduces correlation and minimizes the difference of embeddings. This prevents
581 dimension collapse and also forces the two views to be encoded similarly. Additionally, reducing
582 covariance encourages different dimensions of the representation to capture distinct features.

583 9 Rank and Dormant Neuron

584 [Kumar et al. \(2021\)](#) introduced the concept of *effective rank* for representations, represented as
585 $srank_{\delta}(\phi)$, with δ being a threshold parameter, set to 0.01 as per their study. They proposed that
586 effective rank is linked to the expressivity of a network, where a decrease in effective rank implies
587 an implicit under-parameterization. The study provides evidence indicating that bootstrapping is the
588 primary factor contributing to the collapse of effective rank, which in turn degrades performance.

589 To investigate how SSL objectives might mitigate rank collapse, we computed the rank of the con-
590 volution output and the outputs of the penultimate layers from the advantage and value heads of
591 three different agents: SPR-VICReg, SPR-Barlow, and ZeroJump (SPR without a transition model),
592 scores in [1](#). Our observations indicate that, although there are some rank differences among the
593 agents, they often converge to the same rank, and these differences do not correlate with the perfor-
594 mance scores. [Figure 5](#), [7](#) and [6](#) include ranks across all games.

595 To explore this further, we examined the proportion of dormant neurons, which are neurons that have
596 near-zero activations. [Sokar et al. \(2023\)](#) showed that deep reinforcement learning agents experience
597 a rise in the number of dormant neurons within their networks. Additionally, a higher prevalence of
598 dormant neurons is associated with poorer performance.

599 We also do not observe a clear pattern in the fractions of dormant neurons, in [Figure 8](#) that could
600 account for the disparities in performance scores, similar to what was seen in the case of neuron
601 ranks. Unlike rank-based observations, where patterns may emerge, the distribution of dormant
602 neurons does not offer an explanation for the differences in the scores across models. This suggests
603 that the relationship between neuron activity and performance metrics might be more complex and
604 not directly attributable to the proportion of inactive neurons.

605 10 Experimental Details

606 We retain all hyperparameters of SPR, SR-SPR, and BBF, except for SPR-Barlow and SPR-VICReg,
607 where we adjust the SPR loss weight and increase the batch size from 32 to 64. The official reposi-
608 tories of the models are used, and all experiments are conducted on a Tesla T4 GPU.

609 **11 Full Results on Atari 100k**

Table 3: Returns on the 26 games of Atari 100k after 2 hours of real-time experience, and human-normalized aggregate metrics. (VR: VICReg, results with 5 integral digits are rounded to the first integer to fit the table)

Game	Rand.	Human	Naked	Non	Prio	VR-L	VR-H	Barlow	SPR
Alien	227.8	7127.7	868.9	881.7	872.7	902.9	922.4	891.8	841.9
Amidar	5.8	1719.5	165.6	179.1	164.2	181.1	176.4	177.1	179.7
Assault	222.4	742.0	544.5	564.6	589.2	536.4	575.7	581.4	565.6
Asterix	210	8503.3	972.0	951.0	977.8	955.4	1021.7	981.2	962.5
BankHeist	14.2	753.1	61.6	70.1	60.2	79.9	82.9	73.5	345.4
BattleZone	2360	37188	7552.4	9424.2	13102	12557	14892	14954	14834
Boxing	0.1	12.1	27.3	30.4	36.4	31.3	33.9	35.1	35.7
Breakout	1.7	30.5	16.7	18.0	18.2	16.9	16.3	17.0	19.6
ChopComm	811	7387.8	906.8	949.8	901.0	832.9	929.9	938.9	946.3
CrzyClnbr	10781	35829	30056	32667	35829	27035	29023	29229	36701
DemonAtt	152.1	1971.0	514.7	511.0	522.9	461.2	547.2	519.2	517.6
Freeway	0.0	29.6	17.4	13.71	16.3	28.0	27.7	29.5	19.3
Frostbite	65.2	4334.7	1137.2	1010.9	1014.2	1353.0	1181.4	1191.3	1170.7
Gopher	257.6	2412.5	585.0	660.1	548.4	737.9	713.5	691.2	660.6
Hero	1027	30826	6937.8	6497.8	5686.6	5495.1	5559.6	5746.8	5858.6
Jamesbond	29	302.8	327.2	359.9	349.1	357.6	384.3	404.2	366.5
Kangaroo	52	3035.0	2970.9	2812.1	3016.5	2290.6	1998.3	1771.2	3617.4
Krull	1598	2665.5	3980.4	4061.8	4213.1	4166.6	4513.9	4363.2	3681.6
KFMaster	258.5	22736	13126	14595	15757	1488.4	15548	15998	14783
MsPacman	307.3	6951.6	1262.1	1162.6	1324.6	1366.8	1588.2	1388.2	1318.4
Pong	-20.7	14.6	-1.8	-6.0	-7.2	-6.3	-10.1	-6.7	-5.4
PrivateEye	24.9	69571	85.6	77.0	88.0	100.9	96.6	99.6	86.0
Qbert	163.9	13455	847.2	758.6	759.8	796.9	687.6	765.8	866.3
RoadRunner	11.5	7845.0	12595	12713	11211	10683	9531.5	12412	12213
Seaquest	68.4	42055	524.0	524.2	523.2	576.3	651.0	669.1	558.1
UpNDown	533.4	11693	9569.3	8130.6	10331	7952.7	9415.3	10818	10859
#Sprhmn(\uparrow)	0	N/A	4	3	3	4	4	4	6
Mean (\uparrow)	0.00	1.000	0.542	0.555	0.608	0.558	0.585	0.608	0.616
Median (\uparrow)	0.00	1.000	0.225	0.221	0.308	0.297	0.280	0.312	0.396
IQM (\uparrow)	0.00	1.000	0.273	0.278	0.298	0.292	0.298	0.321	0.337
Opt. Gap (\downarrow)	1.00	0.000	0.617	0.615	0.603	0.609	0.605	0.587	0.577

610 **12 Full Results on DMControl 100k**

Table 4: Returns on the of DMControl 100k, and Max-normalized aggregate metrics.

Environment	Virtual	VICReg+Pred	Barlow+Pred	SPR	VICReg	Barlow
FINGER, SPIN	896.2	760.6	781.0	755.9	730.0	861.8
CARTPOLE, SWINGUP	815.1	791.6	784.0	826.0	780.1	778.6
REACHER, EASY	827.0	790.7	589.6	671.5	736.1	526.5
CHEETAH, RUN	489.6	504.3	461.6	435.2	493.5	478.6
WALKER, WALK	404.7	622.8	521.7	404.7	765.	182.2
BALL IN CUP, CATCH	835.4	891.6	622.8	835.4	937.5	924.9
Mean (\uparrow)	0.705	0.738	0.673	0.660	0.740	0.625
Median (\uparrow)	0.803	0.772	0.703	0.726	0.750	0.652
IQM (\uparrow)	0.744	0.773	0.670	0.677	0.750	0.656
Optimality Gap (\downarrow)	0.294	0.260	0.326	0.339	0.29	0.374

611 **13 Rank and Dormant Neuron Results**

Figure 5: Rank of the output from the penultimate layer of the value head, measured every 10,000 steps and averaged across 10 different runs for every game.

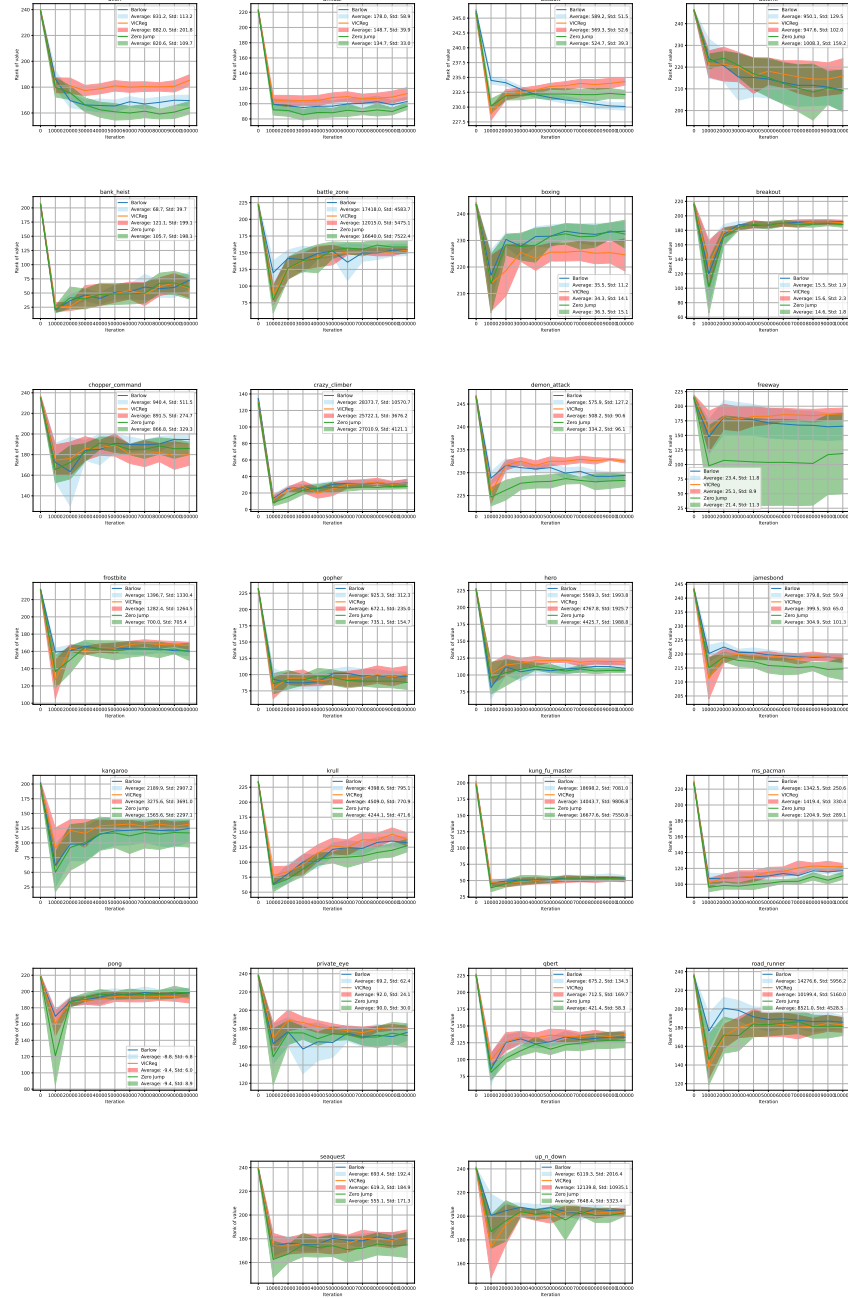


Figure 6: Rank of the output from the convolution encoder, measured every 10,000 steps and averaged across 10 different runs for every game.

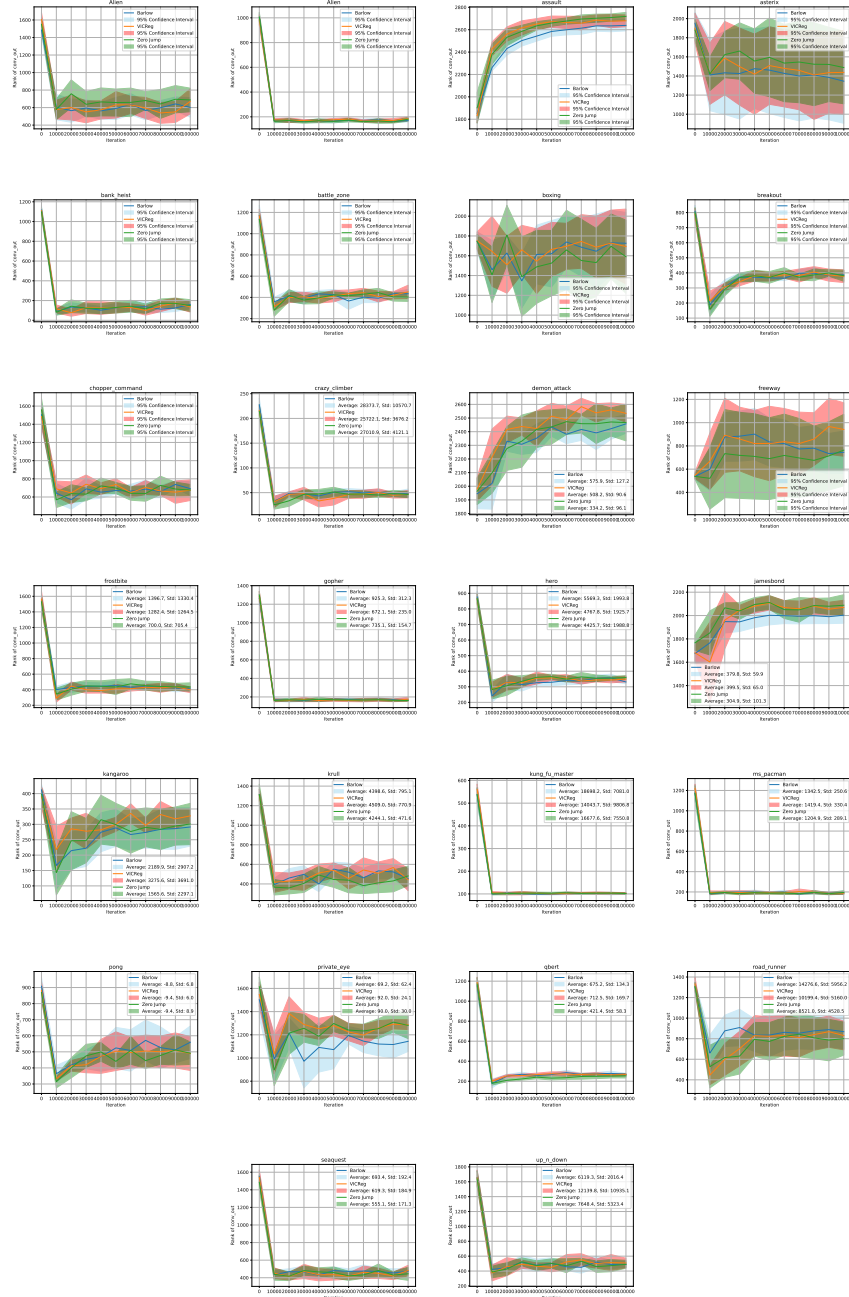


Figure 7: Rank of the output from the penultimate layer of the advantage head, measured every 10,000 steps and averaged across 10 different runs for every game.

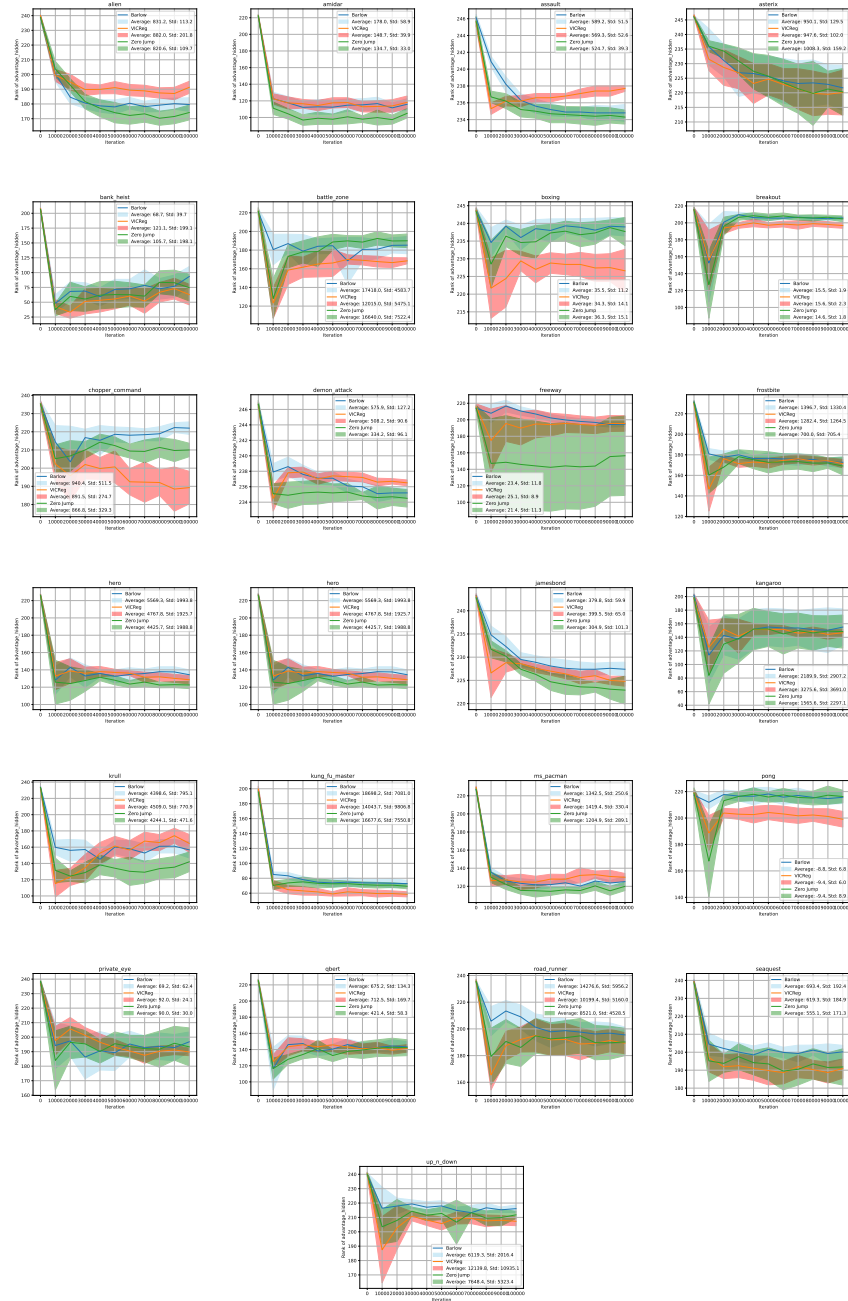


Figure 8: Fraction of dormant neurons averaged across 10 different runs for every game.

